

**FULL PAPER****Applied  
Organometallic  
Chemistry****WILEY**

# High catalytic performance of the first electrospun nano-biohybrid, $\text{Mn}_3\text{O}_4$ /copper complex/polyvinyl alcohol, from *Amaranthus spinosus* plant for biomimetic oxidation reactions

Atena Naeimi<sup>1</sup> | Mehri-Saddat Ekrami-Kakhki<sup>2</sup><sup>1</sup>Department of Chemistry, Faculty of Science, University of Jiroft, Jiroft, 7867161167, Iran<sup>2</sup>Central Research Laboratory, Esfarayen University of Technology, Esfarayen, North khorasan, Iran**Correspondence**Atena Naeimi, Department of Chemistry, Faculty of Science, University of Jiroft, Jiroft 7867161167, Iran.  
Email: a.naeimi@ujiroft.ac.ir

In this study, a novel nano-biocomposite, polyvinylalcohol/ $\text{Mn}_3\text{O}_4$ /water-soluble copper complex (PVA/ $\text{Mn}_3\text{O}_4$ /CuWSC), was produced from *Amaranthus spinosus*. By combining water-soluble copper nanocomplex and  $\text{Mn}_3\text{O}_4$  nanoparticles along with polyvinyl alcohols and extracts of this plant, this bio nanomaterial was prepared via electrospinning process. This nanohybrid was characterized using transmission electron microscopy, scanning electron microscopy, atomic force microscopy, Fourier-transform infrared spectroscopy, X-ray diffraction, energy-dispersive X-ray spectroscopy, and elemental analysis. Based on its catalytic activities, it is considered a heterogeneous catalyst and is used for the oxidation of alcohols in industrial reactions. It can oxidize the primary and secondary alcohols to corresponding aldehyde and ketone products with high yield and excellent selectivity using  $\text{H}_2\text{O}_2$  under solvent-free conditions. The recyclability and reusability of PVA/ $\text{Mn}_3\text{O}_4$ /CuWSC show that it can be a promising catalyst for clean industrial catalytic applications.

**KEY WORDS***Amaranthus spinosus*, bio-nanopolymer, electrospinning, industrial reactions

## 1 | INTRODUCTION

Nowadays, designing novel nanohybrid polymers is generating significant interest due to their wise use in academic and industrial applications.<sup>[1,2]</sup> The scope and utility of these polymers can be further broadened by developing fibers consisting of nano metal oxides and/or transition metal complex for applications in nonwoven surface modification.<sup>[3]</sup> A potential option in this regard is to develop electrospun nanofibers using these materials. Their very high surface-to-volume ratio makes the nanofiber-based polymers well suited for a broad

spectrum of applications, including those related to air filtration, water purification, heterogeneous catalysis, environmental protection, smart textiles, surface coating, energy harvesting/conversion/storage, encapsulation of bioactive species, drug delivery, tissue engineering, and regenerative medicine.<sup>[4–8]</sup> However, preparation of this type of nanomaterials is key for actual industrial applications.<sup>[9,10]</sup> From green chemistry point of view, ultrasonic irradiation and electrospinning can be used for large-scale production, as they are simple and versatile. The morphology of the electrospun fibers is affected by solution properties that include viscosity, conductivity, and

surface tension as well as process parameters that include the flow rate of the precursor solution and electric field intensity. On the contrary, the surface and/or interior of such nanofibers can be further functionalized with molecular species or nanoparticles during or after the electrospinning process to produce the desired product for different applications.<sup>[11–13]</sup>

A weed is an unwanted plant that grows among, and in competition with, cultivated plants. They are undesirable in human-controlled settings such as farm fields, parks, and gardens.<sup>[14]</sup> When one species of plant is valuable, another species from the same genus might be a serious weed; for example, *Amaranthus spinosus* can be a serious weed of rice cultivation in Asia.<sup>[15]</sup> The term “weed” also is applied to any plant that grows or reproduces aggressively or is invasive outside its native habitat. Therefore, weed control is important in agriculture.<sup>[16]</sup> Hand cultivation with hoes, powered cultivation with cultivators, smothering with mulch, lethal wilting with high heat, burning, and chemical attack with herbicides are some of the methods to control them.<sup>[17,18]</sup> On the contrary, weed has many applications, and its ability to produce a novel nanomaterial for different applications has attracted our interest and can solve many challenges in different fields. Our aim was to design a metal-supported biopolymer catalyst based on the weed. Milder operational conditions, low cost, environmental friendliness, and abundance of the weed in nature have gained the attention of the researchers recently.

Selective oxidation of primary and secondary alcohols to carboxylic acids (or aldehydes) and ketones, respectively, is one of the most important transformations in organic synthesis due to the importance of these corresponding carbonyl compounds in the pharmaceutical, agrochemical, and fine and bulk chemical industries.<sup>[19–23]</sup> Catalytic oxidation plays a vital role in speeding up the oxidation of alcohols by reducing the activation energy of the reaction. Many stoichiometric oxidants are associated with toxic and environmentally undesirable heavy metals and high temperatures. Consequently, the development of environmentally friendly methods that use safe, low-cost, and efficient catalytic systems using natural resources is of great research interest in modern green chemistry.

We have extensively explored the use of nanocatalysts for a range of applications.<sup>[24–29]</sup> In this study, Mn<sub>3</sub>O<sub>4</sub> nanoparticles were synthesized using *A. spinosus* weed solution (ASWS), and water-soluble copper nanocomplex (CuWSC) was prepared using ultrasonic irradiation. Mn<sub>3</sub>O<sub>4</sub> nanoparticles and CuWSC along with polyvinyl alcohol (PVA) were applied to obtain fiber-shaped nanocomposite PVA/Mn<sub>3</sub>O<sub>4</sub>/CuWSC through electrospinning technique.

## 2 | EXPERIMENTAL

### 2.1 | Materials and instruments

*A. spinosus* weed was collected from Mahmoodabad village, Jiroft, Iran. Vanillin and Cu(NO<sub>3</sub>)<sub>2</sub> and Mn(NO<sub>3</sub>)<sub>2</sub>·4H<sub>2</sub>O were purchased from Sigma-Aldrich. 9-Aminoacridine and polyvinyl alcohol were purchased from Merck. X-ray diffraction (XRD) pattern of PVA/Mn<sub>3</sub>O<sub>4</sub>/CuWSC was investigated using a Bruker D8-advance X-ray diffractometer with Cu K $\alpha$  ( $k = 0.154$  nm) radiation. Fourier-transform infrared (FT-IR) spectra were recorded using FT-IR spectrophotometer (NICOLET iS10). Thermo stability of PVA/Mn<sub>3</sub>O<sub>4</sub>/CuWSC was determined using a simultaneous thermal analyzer. The nanoparticles of PVA/Mn<sub>3</sub>O<sub>4</sub>/CuWSC were characterized using a transmission electron microscope (Philips CM30). X-ray energy-dispersive spectroscopy (EDAX) detector (IE 300X, Oxford, UK) attached to the scanning electron microscope was used to analyze the elemental composition of materials. An atomic force microscopy (DME Model Igloo) was performed to produce atomic force microscopy (AFM) images of PVA/Mn<sub>3</sub>O<sub>4</sub>/CuWSC. The electrospinning instrument was used for the synthesis of PVA/Fe<sub>2</sub>O<sub>3</sub>/CuWSC (Nanoazma Company, Iran). An ultrasonic cleaner 5200i S3 was used for the synthesis of nanoparticles.

### 2.2 | Green synthesis of Mn<sub>3</sub>O<sub>4</sub> nanoparticles using *A. spinosus* weed

The *A. spinosus* weed extract (ASWE) was prepared by heating 4 g of *A. spinosus* leaves in 50 ml of Milli-Q water at 80 °C for 15 min. After settling for 1 h, the extract was vacuum filtered.

An amount of 200 ml of manganese (II) nitrate tetrahydrate (0.05 M) was added to 170 ml of the extract solution at pH = 6.5 within 15 min at room temperature (KOH, 0.01 M). The resultant brown precipitate was centrifuged and washed with distilled water several times.

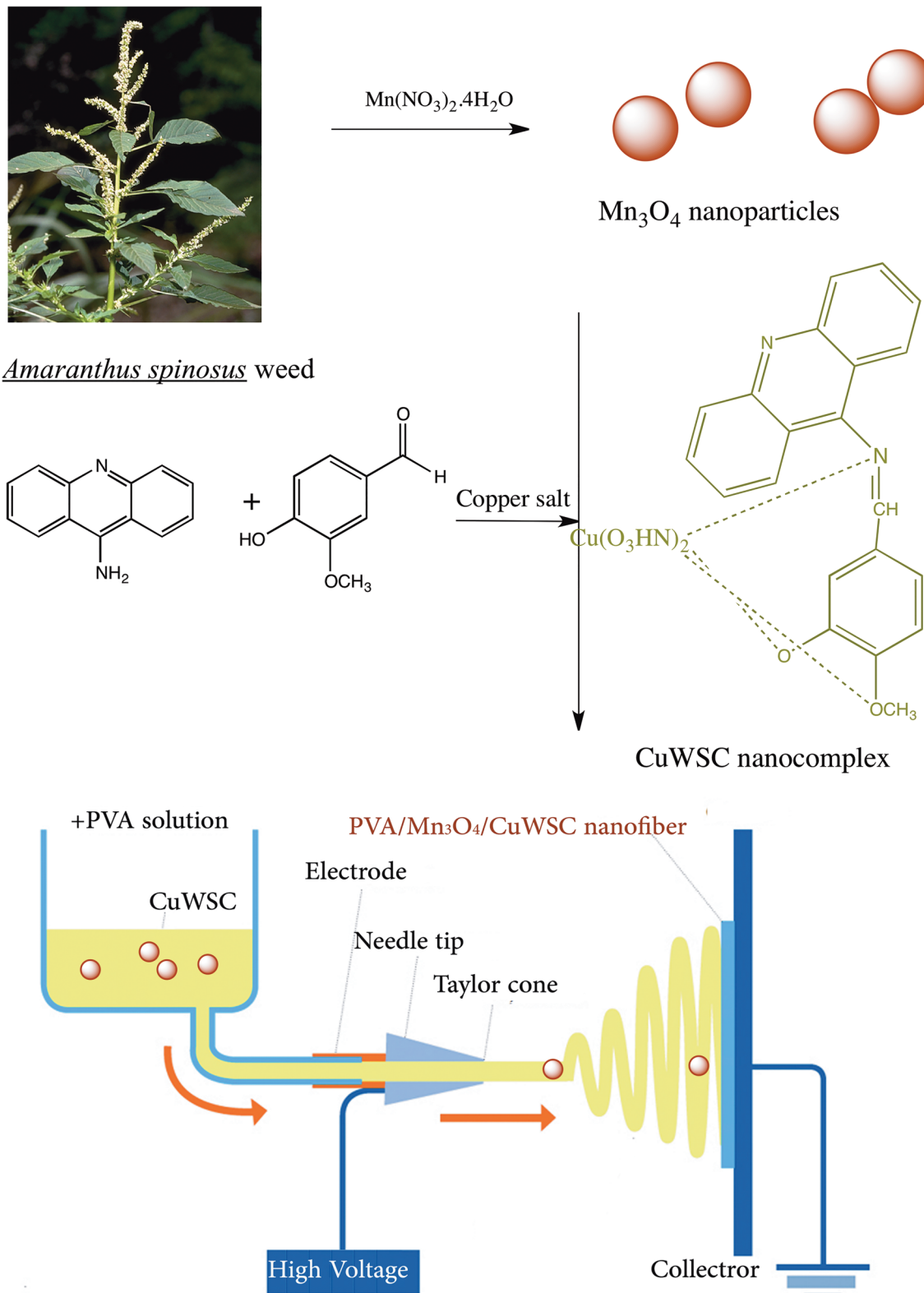
### 2.3 | Synthesis of Schiff base ligand

Schiff base ligand was obtained by adding a solution of vanillin (5 mmol, 0.76 g) in ethanol (20 ml) to a solution of 9-aminoacridine (5 mmol, 0.97 g) in 20 ml ethanol, and the reaction mixture was stirred for 24 h at room temperature. The yellow precipitate obtained was filtered and dried in air.

## 2.4 | Synthesis of water-soluble copper nanocomplex (**CuWSC**)

First 2 mmol of the ligand (0.76 g) was dissolved in THF (10 ml), and then Cu (NO<sub>3</sub>)<sub>2</sub> (2 mmol, 0.38 g)

was dissolved in THF and added to the above solution drop-wise under ultrasonic conditions (400 w, 20 kHz). After 120 min, the green precipitate obtained was filtered, washed with ethanol and THF, and dried in the air.



**SCHM**E 1 The synthesis of PVA/Mn<sub>3</sub>O<sub>4</sub>/CuWSC nanofiber polymer

## 2.5 | Electrospinning procedure of Mn<sub>3</sub>O<sub>4</sub>/water-soluble copper complex (PVA/Mn<sub>3</sub>O<sub>4</sub>/CuWSC)

Mn<sub>3</sub>O<sub>4</sub> (0.1 g) and Cu-WSC (0.1 g) were dissolved in 20 ml of ASWE solution within 30 min and were added to 12 g of PVA in 12 ml of ASWE solution. The reaction mixture was irradiated under ultrasonic conditions for 30 min. The prepared solution was stirred for 8 h at 80 °C. The electrospinning of the final prepared solution was performed at an electrical voltage of 25 kV at room temperature under atmospheric pressure. The polymer fibers were injected using a 5-ml syringe needle having 1.23 mm outer diameter and 0.83 mm internal diameter at a flow rate of 0.3 ml/h. The grounded target was placed at 12 cm from the needle tip.

## 2.6 | Oxidation of alcohols

To a mixture of alcohol (0.2 mmol) and PVA/Mn<sub>3</sub>O<sub>4</sub>/CuWSC nanocomposite (0.14 g) H<sub>2</sub>O<sub>2</sub> was added under solvent-free conditions, and the reaction mixture was stirred at 80 °C for 4h. To this mixture, ethyl acetate

(EtOAc) was added, and the resultant product was filtered (or centrifuged) to remove the catalyst and were purified by plate silica chromatography using *n*-hexane/ethyl acetate (10:2).

## 2.7 | Recycling procedure for oxidation of benzyl alcohol

Benzyl alcohol (0.1 mmol) and PVA/Mn<sub>3</sub>O<sub>4</sub>/CuWSC nanocomposite (0.07 g) were added to H<sub>2</sub>O<sub>2</sub> under solvent-free conditions, and the reaction mixture was stirred under air at 80 °C for 4 h. To the mixture, EtOAc or ethanol was added, and the product was filtered (or centrifuged) and washed again with EtOAc or ethanol. It was dried under vacuum and weighed before use in the next run to avoid errors resulting from the loss of the catalytic activity.

## 3 | RESULTS AND DISCUSSION

Mn<sub>3</sub>O<sub>4</sub>, the Schiff base ligand, CuWSC, and PVA/Mn<sub>3</sub>O<sub>4</sub>/CuWSC nanofibers were synthesized as described earlier in the Experimental section (see Scheme 1).

**FIGURE 1** XRD pattern of PVA/Mn<sub>3</sub>O<sub>4</sub>/CuWSC nano bio-composite

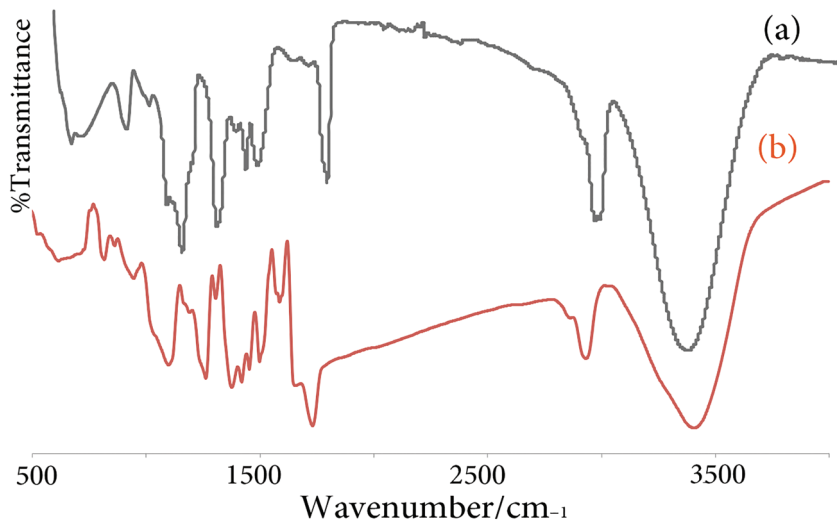
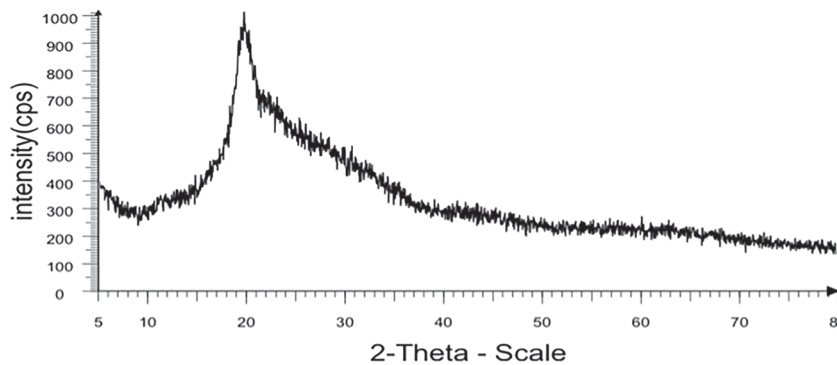


**FIGURE 2** FT-IR of PVA (a) and PVA/Mn<sub>3</sub>O<sub>4</sub>/CuWSC nanofiber (b)

Figure 1 shows the XRD patterns of PVA/Mn<sub>3</sub>O<sub>4</sub>/CuWSC nanofibers. The patterns show strong crystalline reflections at around 20=19.92 and a shoulder at 22.74. The two peaks are characteristic of PVA representing reflections from (101) and (200) from monoclinic unit cells.<sup>[30–32]</sup> It can be seen that the XRD patterns of the nanocomposite have the peaks corresponding to the semi-crystalline nature of pure PVA.<sup>[11]</sup> The existence of OH groups along the main chain of PVA is enough to provide strong intermolecular and intramolecular hydrogen bonding in PVA. The broad peak at 40.7 can be described the amorphous phase in PVA.

FT-IR spectra hint at the structural changes and the possible interaction among PVA and Mn<sub>3</sub>O<sub>4</sub> and CuWSC nanocomplex (Figure 2a,b). The absorption peaks of PVA included 3241 cm<sup>-1</sup> (stretching of OH), 2935 cm<sup>-1</sup> (symmetric stretching of CH<sub>2</sub>), 1426 cm<sup>-1</sup> (bending of OH and wagging of CH<sub>2</sub>), 1321 cm<sup>-1</sup> (stretching of C=O), and 1073 cm<sup>-1</sup> (stretching of CO and bending of OH from the amorphous sequence of

PVA).<sup>[33,34]</sup> Figure 2b shows the spectrum of nanofibers obtained from Mn<sub>3</sub>O<sub>4</sub>/CuWSC and PVA polymer. The presence of Mn<sub>3</sub>O<sub>4</sub> nanoparticles in the fibers can be verified by the observation of new characteristic peaks (730 cm<sup>-1</sup>) corresponding to the frequencies associated with the stretching metal-oxygen of metal oxide nanoparticles. The peak observed at 736.81 cm<sup>-1</sup> may be attributed to the O atoms in the Mn-O layers.<sup>[35]</sup> The peak at 817.82 and 852.54 cm<sup>-1</sup> may be due to overtone modes of bulk Mn-O stretching's Mn<sub>3</sub>O<sub>4</sub>.<sup>[36]</sup> The strong band at 1631 cm<sup>-1</sup> was due to C=N of imine, indicating the presence of the Schiff base ligands. The new peaks at 1500 and 1517 cm<sup>-1</sup> were related to the benzene ring conjugated to the imine group in nanocomplex.

The neat electrospun PVA fiber webs as well as the electrospun PVA/Mn<sub>3</sub>O<sub>4</sub>/CuWSC fiber webs were prepared to compare the differences in appearance between them. Scanning electron microscopy (SEM) images of the neat PVA and PVA/Mn<sub>3</sub>O<sub>4</sub>/CuWSC electrospun nanofibers are shown in Figure 3. The SEM image of

**FIGURE 3** SEM images of (a) PVA polymer and (b) PVA/Mn<sub>3</sub>O<sub>4</sub>/CuWSC nanobiocomposite

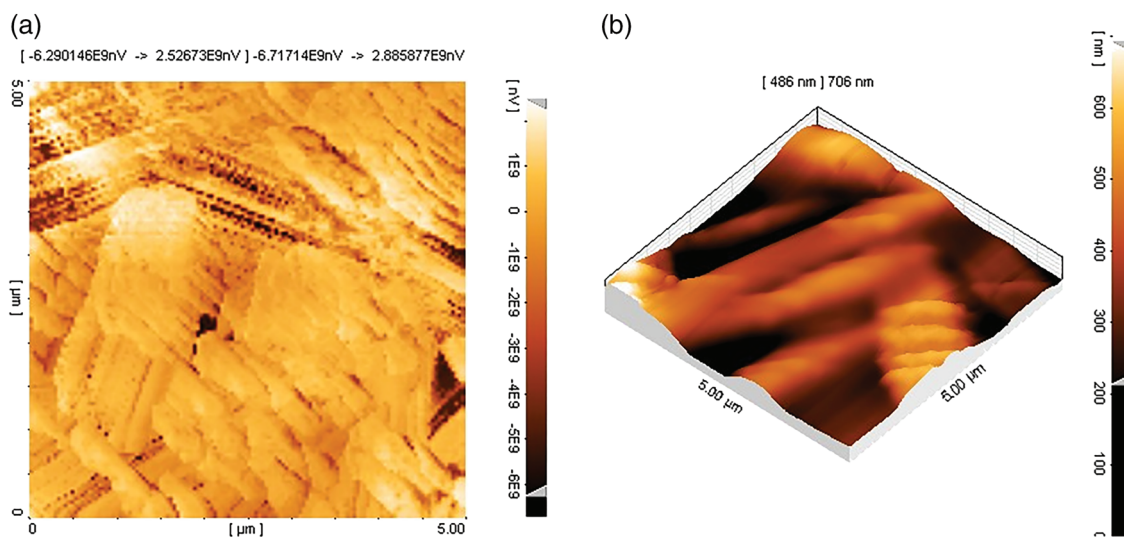
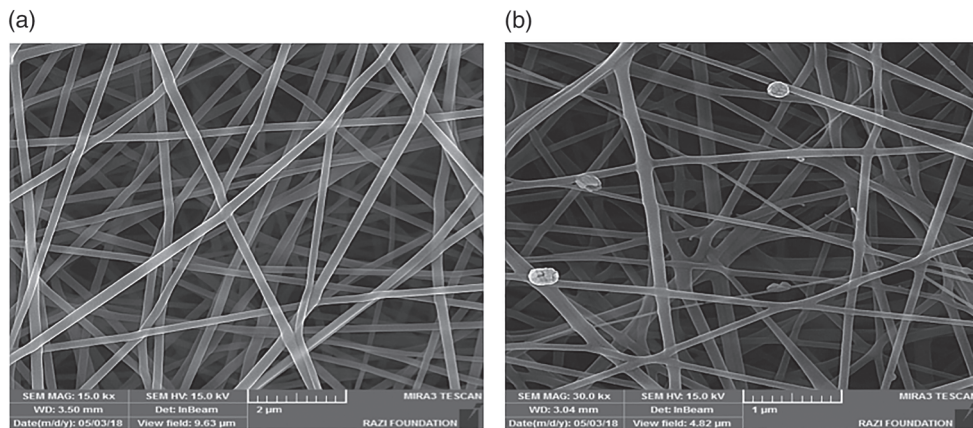


**FIGURE 4** (a) Two- and (b) three-dimensional AFM images of PVA/Mn<sub>3</sub>O<sub>4</sub>/CuWSC

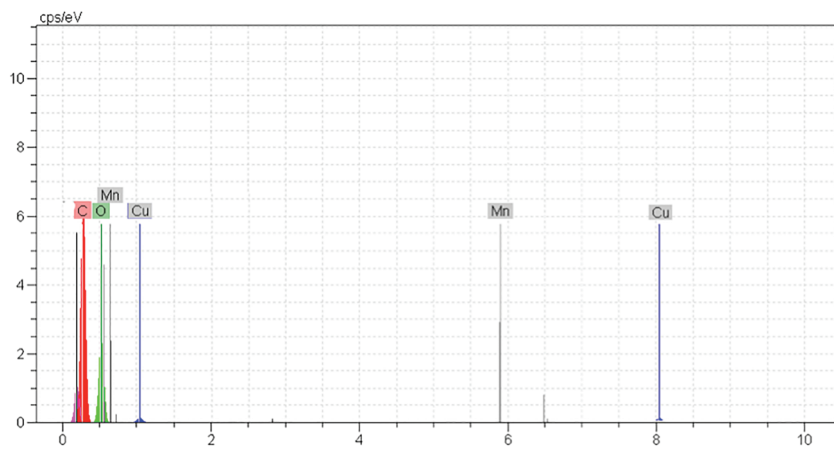


**FIGURE 5** EDAX of PVA/Mn<sub>3</sub>O<sub>4</sub>/CuWSC nanofiber

PVA confirmed the cylindrical shape of nanotubes having the average crystallite size of 40 nm. SEM image of electrospun PVA/Mn<sub>3</sub>O<sub>4</sub>/CuWSC nanofibers confirmed the Mn<sub>3</sub>O<sub>4</sub> nanoparticles and CuWSC nanocomplex in this bio-nanocomposite. The cylindrical shape without aggregation was also confirmed by the SEM images. This characteristic enables soluble CuWSC and Mn<sub>3</sub>O<sub>4</sub> nanoparticles to be uniformly dispersed in the PVA matrix.<sup>[37]</sup> The fibril structure of this natural

**TABLE 1** The elemental analysis of PVA/Mn<sub>3</sub>O<sub>4</sub>/CuWSC nanofiber

| Entry | Elements  | Weight % | Atomic% |
|-------|-----------|----------|---------|
| 1     | Carbon    | 51.90    | 59.13   |
| 2     | Oxygen    | 47.29    | 40.45   |
| 3     | Sodium    | 0.66     | 0.39    |
| 4     | Manganese | 0.09     | 0.02    |
| 5     | Copper    | 0.06     | 0.01    |

nanocomposite was confirmed by two-dimensional (Figure 4a) and three-dimensional (Figure 4b) AFM topography images.

Energy-dispersive X-ray spectroscopic and elemental analysis showed the presence of Mn and Cu in this bio-nanocomposite and confirmed the Mn<sub>3</sub>O<sub>4</sub> nanoparticles and copper nanocomplex in this nanohybrid, respectively (Figure 5). The weight and atomic percentage of PVA/Mn<sub>3</sub>O<sub>4</sub>/CuWSC are found in Table 1. The high amounts of carbon and oxygen are related to the presence of PVA in this sample.<sup>[24]</sup>

Finally, the transmission electron microscopy images of PVA/Mn<sub>3</sub>O<sub>4</sub>/CuWSC showed the PVA nanofiber containing Mn<sub>3</sub>O<sub>4</sub> and CuWSC (Figure 6). Mn<sub>3</sub>O<sub>4</sub> and CuWSC nanoparticles were well embedded in the nanofibers during the electrospinning process. In fact, there was no effect on its fibril morphology with the blending of these nanoparticles in the PVA solution. The presence of these nanoparticles in the PVA/Mn<sub>3</sub>O<sub>4</sub>/CuWSC nanofibers was confirmed by the EDAX analysis.

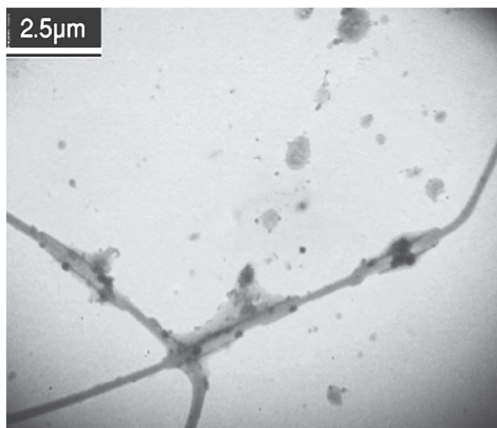


**FIGURE 6** TEM image of PVA/Mn<sub>3</sub>O<sub>4</sub>/CuWSC bio-nanocomposite

### 3.1 | Oxidation of alcohols catalyzed by PVA/Mn<sub>3</sub>O<sub>4</sub>/CuWSC bio-nanocomposite

The catalytic activity of PVA/Mn<sub>3</sub>O<sub>4</sub>/CuWSC bio-nanocomposite was examined in the oxidation of benzyl alcohol using H<sub>2</sub>O<sub>2</sub> as an ideal oxidant (Scheme 2). Reactions carried out with blanks showed no benzyl alcohol conversion at different conditions. The reaction was then carried out using PVA/Mn<sub>3</sub>O<sub>4</sub>/CuWSC bio-nanocomposite as a green catalyst in different solvents, at various temperatures, and using various amounts of H<sub>2</sub>O<sub>2</sub> and the catalyst. Data in entries 1–4 in Table 2 reflect green reaction media effects on catalytic performance: the 45 and 100% benzaldehyde yields were obtained in EtOAc and solvent-free conditions, respectively, at 80°C, whereas EtOH and water only gave a low conversion and yield (15 and 0%, respectively). Therefore, solvent-free conditions were applied as ideal green media for further studies. The reaction exhibited the highest product yield (100%, entry 1) and the corresponding yields decreased at lower temperature (entries 5–9).

Screening of the PVA/Mn<sub>3</sub>O<sub>4</sub>/CuWSC bio-nanocomposite and H<sub>2</sub>O<sub>2</sub> amounts on the catalytic performance was further set of experiments. Data in entries 1–6 in Table 3 show the effect of the applied catalyst in different amounts on the oxidation of benzyl alcohol to benzaldehyde. After 4 h, the reaction reached an almost-quantitative conversion of benzyl alcohol (entries 1–4). The best conversion of oxidation reaction was obtained using 0.07 g of catalyst. Nevertheless, increasing the catalyst loading from 0.01 to 0.1 g led to a significant decrease in the yields from 30 to 10% (entries 4 and 5).

**TABLE 2** The effect of solvent and temperature on the oxidation of benzyl alcohol catalyzed by PVA/Mn<sub>3</sub>O<sub>4</sub>/CuWSC bio-nanocomposite using H<sub>2</sub>O<sub>2</sub><sup>a</sup>

| Entry | Solvent          | Temperature (°C) | Yield of benzaldehyde (%) |
|-------|------------------|------------------|---------------------------|
| 1     | Free solvent     | 80               | 100                       |
| 2     | EtOH             | 80               | 15                        |
| 3     | H <sub>2</sub> O | 80               | –                         |
| 4     | EtOAc            | 80               | 45                        |
| 5     | Free solvent     | 70               | 85                        |
| 6     | Free solvent     | 60               | 70                        |
| 7     | Free solvent     | 50               | 40                        |
| 8     | Free solvent     | 40               | Trace                     |
| 9     | Free solvent     | 25               | –                         |

<sup>a</sup>The reactions were carried out for 4 h in 0.4 ml solvent, H<sub>2</sub>O<sub>2</sub> (0.2 mmol), and catalyst (0.07 g)

On the contrary, other common terminal oxidants, including H<sub>2</sub>O<sub>2</sub> (30%), *tert*-butyl hydroperoxide (TBHP, 70%), urea–hydrogen peroxide (UHP), Oxone®, O<sub>2</sub>, and NaIO<sub>4</sub>, produced benzaldehyde in low yields: 100, 80, 45, 5, 0 and 15%, respectively within 4 h (entries 1–6 in Table 4). The time course study of benzyl alcohol oxidation was investigated under the optimized condition. As shown in Table 4, the conversion of benzyl alcohol sharply increased with an increase in the reaction time from 0.5 to 4 h (entries 7–10).

The ability of other catalysts to promote the oxidation of benzyl alcohol under the optimized condition was probed (Figure 7). Simple copper and manganese salts exhibited poor activity under optimized conditions

**SCHEME 2** The green oxidation of alcohols catalyzed by PVA/Mn<sub>3</sub>O<sub>4</sub>/CuWSC bio-nanocomposite using H<sub>2</sub>O<sub>2</sub>

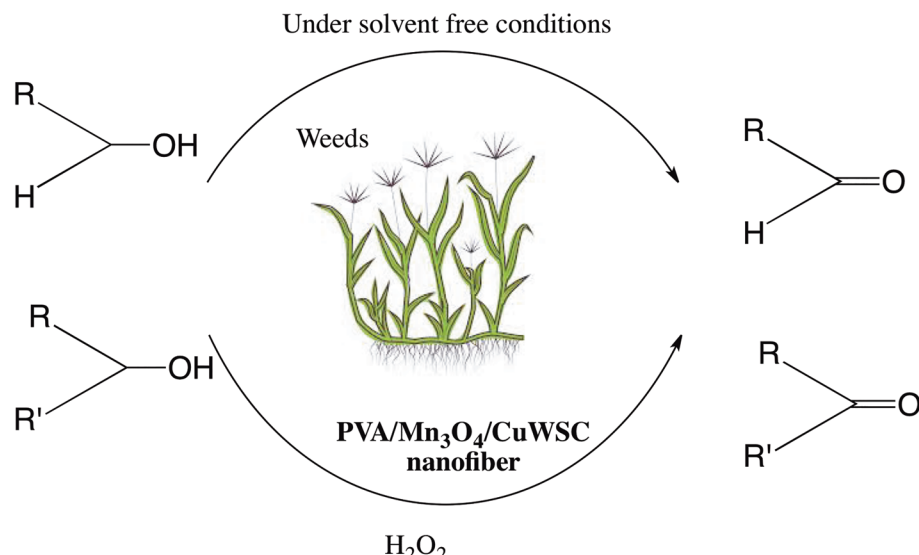


**TABLE 3** The effect of different amounts of catalyst and oxidant on the oxidation of benzyl alcohol

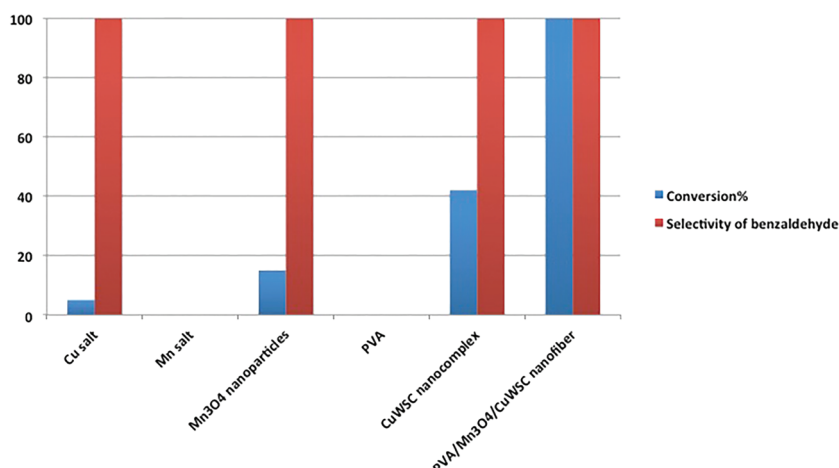
| Entry | Catalyst amount (g) | H <sub>2</sub> O <sub>2</sub> amount (mmol) | Yield (%) |
|-------|---------------------|---|-----------|
| 1     | 0.04                | 0.2   | 50        |
| 2     | 0.06                | 0.2   | 85        |
| 3     | 0.07                | 0.2   | 100       |
| 4     | 0.01                | 0.2   | 30        |
| 5     | 0.1                 | 0.2   | 10        |
| 6     | 0.07                | 0.15  | 90        |
| 7     | 0.07                | 0.1   | 75        |
| 8     | 0.07                | 0.01  | 45        |

<sup>a</sup>The reactions were carried out at 80 °C under solvent-free conditions for 4 h, with 0.1 mmol benzyl alcohol.

**TABLE 4** The effect of time and different types of oxidants on the oxidation of benzyl alcohol

| Entry | Oxidant                       | Time (h) | Yield of benzaldehyde (%) |
|-------|-------------------------------|----------|---------------------------|
| 1     | H <sub>2</sub> O <sub>2</sub> | 4        | 100                       |
| 2     | TBHP                          | 4        | 80                        |
| 3     | UHP                           | 4        | 45                        |
| 4     | Oxone@                        | 4        | 5                         |
| 5     | O <sub>2</sub>                | 4        | –                         |
| 6     | NaIO <sub>4</sub>             | 4        | 15                        |
| 7     | H <sub>2</sub> O <sub>2</sub> | 0.5      | 20                        |
| 8     | H <sub>2</sub> O <sub>2</sub> | 1        | 40                        |
| 9     | H <sub>2</sub> O <sub>2</sub> | 2        | 75                        |
| 10    | H <sub>2</sub> O <sub>2</sub> | 3        | 80                        |

<sup>a</sup>The reactions were carried out at 80 °C at different time intervals up to 4 hours under air and solvent-free conditions. Benzyl alcohol (0.1 mmol), oxidant (0.2 mmol), and catalysts (0.07 g) were used.



(0 and 5%). Figure 7 indicates the activity rate of Mn<sub>3</sub>O<sub>4</sub> nanoparticles, electrospun PVA, and CuWSC nanocomplex. They were actually inactive catalysts for this green strategy.

Thus, with respect to the aforementioned results, to achieve the best results in the oxidation of benzyl alcohol, 0.07 g of the catalyst and 0.2 mmol of H<sub>2</sub>O<sub>2</sub> (30%) was stirred at 80 °C under solvent-free conditions for 4 h, leading to 100% benzaldehyde. Finally, a number of secondary and primary benzylic alcohols were oxidized smoothly to their corresponding ketones (Table 5, entries 1–3) and aldehyde products (Table 5, entries 4–12) regardless of the electronic and steric nature of the arene substituent. The formation of benzoic acids and esters by-products was completely controlled, and desired aldehyde and ketones were obtained in yields ranging from 65% to 100%. However, the catalytic system oxidized secondary alcohols to the corresponding ketones under the same condition with good conversion and excellent selectivity (entries 1–4). Further, the treatment of OH group along with SH group under the optimized conditions for 4 h gave only 100% aldehyde product indicating that our conditions were not amenable for S–H activation (entry 5). Nevertheless, aryl ring substituted with electron withdrawing such as chloro and nitro group (entries 11 and 12) did reduce the conversion of the starting material resulting from the decrease in the spin density on OH group.

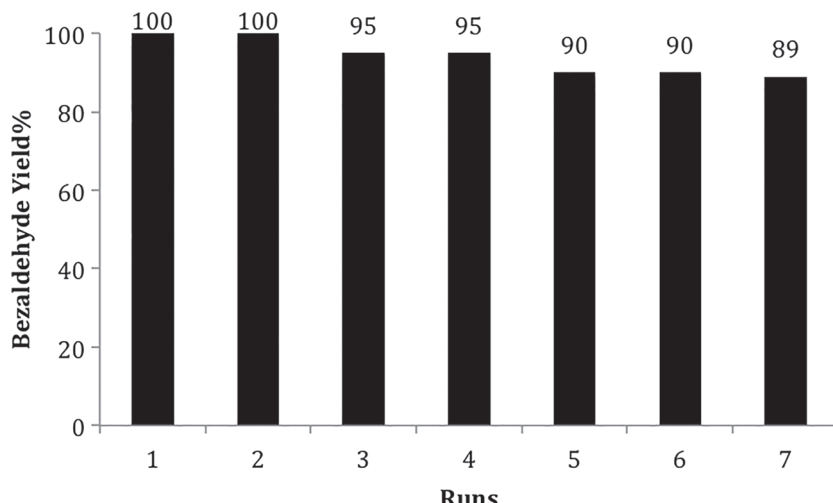
These promising results for the use of PVA/Mn<sub>3</sub>O<sub>4</sub>/CuWSC as a heterogeneous catalyst encouraged us to screen its recyclability in the oxidation of benzyl alcohol. The solid catalyst recovered after a simple washing with ethyl acetate and filtered could be reused multiple times and showed only 11% reduction in the yield of benzaldehyde product even after seven runs (Figure 8).

**FIGURE 7** The effect of different catalysts on the transformation of benzyl alcohol to benzaldehyde

**TABLE 5** The oxidation of different alcohols catalyzed by PVA/Mn<sub>3</sub>O<sub>4</sub>/CuWSC bio-nanocomposite using H<sub>2</sub>O<sub>2</sub> (30%)

| Entry | Alcohol | Product | Yield of product (%) |
|-------|---------|---------|----------------------|
| 1     |         |         | 65                   |
| 2     |         |         | 95                   |
| 3     |         |         | 60                   |
| 4     |         |         | 90                   |
| 5     |         |         | 100                  |
| 6     |         |         | 100                  |
| 7     |         |         | 100                  |
| 8     |         |         | 100                  |
| 9     |         |         | 100                  |
| 10    |         |         | 100                  |
| 11    |         |         | 95                   |
| 12    |         |         | 90                   |

<sup>a</sup>The reactions of entries 1–14 were carried out at 80 °C under air and solvent-free conditions using 0.1 mmol substrate with 0.07 g catalyst and 0.2 mmol H<sub>2</sub>O<sub>2</sub> (30%).

**FIGURE 8** The reusability of PVA/Mn<sub>3</sub>O<sub>4</sub>/CuWSC nanofiber for oxidation of benzyl alcohol

## 4 | CONCLUSION

To conclude, for the first time  $Mn_3O_4$  nanoparticles and electrospun PVA/ $Mn_3O_4$ /CuWSC nanofiber were synthesized from Amaranthus spinosus. PVA/ $Mn_3O_4$ /CuWSC nanofiber is the first catalyst based on a weed that is used as an efficient industrial catalyst for the selective oxidation of primary and secondary alcohols. The high activity and survival of this catalyst could provide high yielding methods for producing desired aldehyde or ketone compounds. Nanofibers with excellent reusability synthesized under solvent-free conditions, using ethyl acetate as a safe solvent and  $H_2O_2$  as an ideal oxidant show great potential for real environmental and industrial applications.

## ACKNOWLEDGMENT

We are thankful to Iran National Science Foundation (INSF) for its support on this work.

## ORCID

Atena Naeimi  <https://orcid.org/0000-0001-6328-7342>

## REFERENCES

- [1] Z. M. Huang, Y. Z. Zhang, M. Kotaki, S. Ramakrishna, *Compos. Sci. Technol.* **2003**, 63, 2223.
- [2] S. Talwar, A. S. Krishnan, J. P. Hinestroza, B. Pourdeyhimi, S. A. Khan, *Macromolecules* **2010**, 43, 7650.
- [3] J. Xue, J. Xie, W. Liu, Y. Xia, *Acc. Chem. Res.* **2017**, 50, 1976.
- [4] S. Jiang, Y. Chen, G. Duan, C. Mei, A. Greiner, S. Agarwal, *Polym. Chem.* **2018**, 9, 2685.
- [5] H. D. Zhang, Y. J. Liu, J. Zhang, J. W. Zhu, Q. H. Qin, C. Z. Zhao, X. Li, J. C. Zhang, Y. Z. Long, *J. Phys. D Appl. Phys.* **2018**, 51, 085102.
- [6] V. Palaninathan, S. Raveendran, A. K. Rochani, N. Chauhan, Y. Sakamoto, T. Ukai, T. Maekawa, D. S. Kumar, *J. Tissue Eng. Regen. Med.* **2018**, 12, 1634.
- [7] M. Venkatram, H. N. R. N. Murthy, A. Gaikwad, S. A. Mankunipoyil, S. Ramakrishna, P. A. Ratna, *Closing and textile Journal* **2018**, 36, 296.
- [8] C. Kenry, T. Lim, *Progress in Polymer Science* **2017**, 70(1).
- [9] T. Jiang, E. J. Carbone, K. W. H. Lo, C. T. Laurencin, *Prog. Polym. Sci.* **2015**, 46, 1.
- [10] X. Yang, W. Zou, Y. Su, Y. Zhu, H. Jiang, J. Shen, C. Li, *J. Power Sources* **2014**, 266, 36.
- [11] S. Agarwal, A. Greiner, J. H. Wendorff, *2013*, 38, 963.
- [12] D. Chen, S. K. Sharma, A. Modhoo, *Handbook on Applications of Ultrasound: Sonochemistry for Sustainability*, CRC Press, Boca Raton, FL **2012**.
- [13] R. Radhakrishnan, A. A. Alqarawi, E. F. A. Allah, *Ecotoxicol. Environ. Saf.* **2018**, 158, 131.
- [14] B. P. Caton, M. Mortimer, J. E. Hill, D. E. Johnson, *A practical field guide to weeds of rice in Asia*, Second Edition, Los Baños (Philippines) **2010**.
- [15] E. Pannacci, F. Tei, M. Guiducci, *Crop Prot.* **2018**, 104, 52.
- [16] M. Tu, C. Hurd, J. M. Randall, *Weed Control Methods Handbook: Tools & Techniques for Use in Natural Areas, Wild and Invasive Species Team version April 2001*
- [17] C. Redlick, L. D. Syrový, H. S. N. Duddu, D. Benaragama, E. N. Johnson, C. J. Willenborg, S. J. Shirtliffe, *Weed Sci.* **2017**, 65, 778.
- [18] K. Lagerblom, J. Keskkäväli, A. Parviainen, J. Mannisto, T. Repo, *Chem Cat Chem* **2018**, 10, 2908.
- [19] S. Shirase, K. Shinohara, H. Tsurugi, K. Mashima, *ACS Catal.* **2018**, 8, 6939.
- [20] H. Ünver, I. Kani, *J. Chem. Sci.* **2018**, 130, 33.
- [21] M. N. Kopylovich, A. Ribeiro, E. Alegria, A. J. L. Pombeiro, *Advances in Organometallic Chemistry* **2015**, 63, 91.
- [22] K. P. R. Castro, M. A. S. Garcia, W. C. Abreu, S. A. Sousa, C. V. Moura, J. S. Costa, E. M. Moura, *Catalysts* **2018**, 8, 83.
- [23] S. Abbaspour Noghi, A. Naeimi, H. Hamidian, *Polymer* **2018**, 149, 229.
- [24] A. Sedri, A. Naeimi, S. Z. Mohammadi, *Carbohydr. Polym.* **2018**, 199, 236.
- [25] A. Naeimi, M. Honarmand, A. Sedri, *Ultrason. Sonochem.* **2019**, 50, 331.
- [26] A. Naeimi, A. Amiri, Z. Ghasemi, **2017**, 80, 107.
- [27] A. Lopez-Moreno, D. Clemente-Tejeda, J. Calbo, A. Naeimi, F. A. Bermejo, E. Orti, E. M. Perez, **2014**, 50, 9372.
- [28] E. Tajik, A. Naeimi, A. Amiri, *Cellul.* **2018**, 25, 915.
- [29] S. B. Yang, S. H. Yoo, J. Seok Lee, J. W. Kim, J. H. Yeum, **2017**, 9, 493.
- [30] S. Peng, M. Zhou, F. Liu, C. Zhang, X. Liu, J. Liu, L. Zou, J. Chen, *R. Soc. Open Sci.* **2017**, 4, 170512.
- [31] N. Jaipakdee, T. Pongjanyakul, E. Limpongsa, *Int. J. App. Pharm.* **2018**, 10, 115.
- [32] H. Hu, J. H. Xin, H. Hu, L. He, *Carbohydr. Polym.* **2013**, 91, 305.
- [33] L. H. Fu, S. M. Li, J. Bian, M. G. Ma, X. L. Long, X. M. Zhang, S. J. Liu, *Carbohydr. Polm.* **2015**, 115, 373.
- [34] S. H. Park, W. J. Lee, J. Power, *Sources* **2015**, 281, 301.
- [35] M. Aslam, M. A. Kalyar, Z. A. Raza, *Polym. Eng. Sci.* **2018**, 58, 2119.
- [36] W. Song, X. Yu, D. C. Markel, T. Shi, W. Ren, *Biofabrication* **2013**, 5, 035006.
- [37] V. Thavasi, G. Singh, S. Ramakrishna, *Energ. Environ. Sci.* **2008**, 1, 205.

**How to cite this article:** Naeimi A, Ekrami-Kakhki M-S. High catalytic performance of the first electrospun nano-biohybrid,  $Mn_3O_4$ /copper complex/polyvinyl alcohol, from *Amaranthus spinosus* plant for biomimetic oxidation reactions. *Appl Organometal Chem.* 2020;e5453. <https://doi.org/10.1002/aoc.5453>